Limnol. Oceanogr., 52(5), 2007, 1800–1808

The physicochemical speciation of dissolved iron in the Bering Sea, Alaska

Kristen N. Buck[1]
Scripps Institution of Oceanography, University of California San Diego, La Jolla, California 92093-0218

Kenneth W. Bruland
Department of Ocean Sciences, University of California Santa Cruz, Santa Cruz, California 95064

Abstract

The physicochemical speciation of dissolved iron (Fe) across natural dissolved Fe gradients in the oceanic and shelf domains of the southeastern Bering Sea was examined in surface and subsurface samples using competitive ligand exchange–adsorptive cathodic stripping voltammetry with the added ligand salicylaldoxime. Two ligand classes were measured in all samples, a stronger L_1 ligand class and a weaker L_2 ligand class. Conditional stability constants for both ligand classes were comparable between surface and subsurface samples, with mean log $K^{cond}_{FeL_1,Fe'} = 11.5 \pm 0.3$ and mean log $K^{cond}_{FeL_2,Fe'} = 10.3 \pm 0.3$ in surface samples, and mean log $K^{cond}_{FeL_1,Fe'} = 11.4 \pm 0.2$ with a weaker ligand and mean log $K^{cond}_{FeL_2,Fe'}$ of 10.2 ± 0.2 in subsurface samples. The concentrations of dissolved Fe were strongly correlated with ambient stronger L_1 ligand concentrations for all samples with dissolved Fe concentrations greater than 0.2 nmol L^{-1}. In samples with dissolved Fe concentrations less than 0.2 nmol L^{-1}, large and variable excesses of L_1 ligand concentrations were measured, coincident with observed Fe stress or limitation on the ambient phytoplankton. These observations suggest that the phytoplankton community is readily able to access dissolved Fe from the FeL_1 complex, resulting in excess L_1 in these waters. The available speciation data from other sources indicate that a significant correlation exists between dissolved Fe and L_1 ligand concentrations in samples with intermediate dissolved Fe, and this is a seemingly ubiquitous feature of dissolved Fe cycling in the marine environment.

The Bering Sea consists of a large semienclosed sea, covering nearly 3 million km² in area. Within the Bering Sea are two distinct bathymetric features: a deep (3,000–4,000 m) abyssal basin in the west and a broad (500–800 km wide) shallow (average depth 50–75 m) continental shelf in the east, separated by an abrupt shelf break with a steep continental slope. The continental shelf region constitutes more than half of the surface area of the Bering Sea and is largely responsible for the high productivity reported for the region (Sukhanova et al. 1999).

Three hydrographic regimes are formed by tidal and wind forcing across the southeastern Bering Sea shelf region in the summer (Coachman and Charnell 1979; Fig. 1). The inner shelf domain, shoreward of the 50-m isobath, is vertically well mixed. This domain has also been referred to as the coastal domain (Aguilar-Islas et al. 2007). The middle shelf domain is generally found between the 50-m and 100-m isobaths, and is distinguished by a two-layer water column. The outer shelf domain defines the three-layer regime beyond the 100-m isobath and out to the shelf break. These three distinct hydrographic regimes are separated by frontal systems: the inner front (~50-m isobath) between the inner and middle shelf domains, the middle (~100-m isobath) front between the middle and outer shelf domains, and the shelf break front (~200-m isobath) separating the outer shelf domain from the oceanic domain of the deep Bering Sea basin.

Summer productivity in the Bering Sea is well characterized, and is generally comprised of low productivity in the surface oceanic domain, elevated and sustained productivity at the shelf break, and decreasing productivity moving shoreward from the shelf break (Springer et al. 1996). Macronutrient concentrations in the surface oceanic domain are sufficiently high to support the growth of large (>10 μm) diatoms in the Bering Sea basin, and yet picoplankton generally dominate the phytoplankton community, contributing about 50% of the total biomass (Shiomoto 1999; Sukhanova et al. 1999), although these picoplankton appear to grow much more slowly than the large diatoms in the Bering Sea basin (Liu et al. 2002). Dissolved Fe concentration measurements and results from Fe-amended incubation experiments conducted in the western Bering Sea gyre have indicated that this oceanic region of the Bering Sea is a classic high-nutrient lower-chlorophyll (HNLC) area (Leblanc et al. 2005; Peers et al. 2005; Aguilar-Islas et al. 2007), where large diatom growth is limited by the extremely low (<0.1 nmol L^{-1}) surface-dissolved Fe concentrations (Aguilar-Islas et al. 2007).

In contrast, the shelf region of the eastern Bering Sea is limited by depleted nitrate concentrations during the summer (<0.1 μmol L^{-1}; Aguilar-Islas et al. 2007) following macronutrient drawdown by the initial spring diatom bloom (Whitledge and Luchin 1999). Dissolved Fe concentrations in shelf waters are highest in the bottom

[1] Corresponding author (kbuck@ucsd.edu).

Acknowledgments

We thank Ana Aguilar-Islas and Matthew Hurst for dissolved Fe concentration data, Geoffrey Smith for sampling assistance, and Bettina Sohst for nitrate data. Russ Flegal, Ana Aguilar-Islas, and Raphe Kudela provided insightful comments during the preparation of this manuscript. We also thank three anonymous reviewers for their helpful comments.

This work was funded from an Ida Benson Lynn Graduate Fellowship in Ocean Health and NSF grants OCE-0137085 and OCE-0526601.

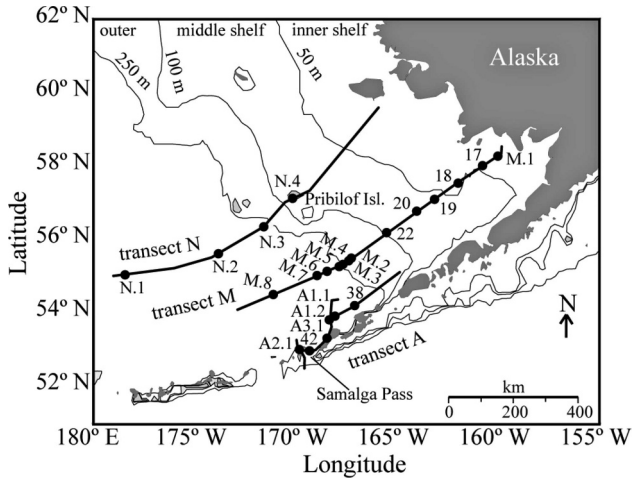

Fig. 1. Adapted from Aguilar-Islas et al. (2007) Fig. 1. Surface speciation sample stations in the southeastern Bering Sea along transect N (N.1–N.4), transect M (M.1–M.8), and transect A (A1.1, A1.2, A2.1, A3.1) as well as subsurface speciation stations along transect M (17–20, 22) and transect A (38, 42).

layers (3.7–12.9 nmol L^{-1}), with surface waters indicating a natural Fe concentration gradient (0.1–3.5 nmol L^{-1}) from the shelf break to the inner shelf domain (Aguilar-Islas et al. 2007). Dissolved manganese (Mn) concentrations also follow a gradient (~5–~36 nmol L^{-1}) across the shelf domains of the Bering Sea, serving to trace continental Fe sources and distinguish hydrographic domains (Aguilar-Islas et al. 2007).

At the outer edge of the southeastern Bering Sea shelf, a region of elevated primary production persists throughout the summer, creating a ''Green Belt'' of high chlorophyll (Springer et al. 1996). The prolonged biological production in the Green Belt is fueled by the increased exchange of macronutrients that occurs from macronutrient-rich basin waters at the shelf break (Stabeno et al. 1999; Whitledge and Luchin 1999; Aguilar-Islas et al. 2007). Additionally, macronutrients from the Aleutian Island passes, brought to the surface by deep mixing characteristic of these passes (Mordy et al. 2005), support the Green Belt at its southern end (Aguilar-Islas et al. 2007).

Dissolved Fe concentrations in the Green Belt are low (~0.1 nmol L^{-1}), and some Fe limitation of the ambient diatom community has been suggested by the slope of measured changes in Si : N ratios ($\Delta Si : \Delta N$) through the upper 80 m of the water column, while assuming subsurface waters were the primary source of these macronutrients and surface production the primary sink (Aguilar-Islas et al. 2007). The main source of dissolved Fe to the Green Belt appears to be from the Pribilof Island domain in the north and the Bering Canyon and Aleutian Island passes in the south.

In the vicinity of the Pribilof Islands, a well-mixed coastal domain surrounds each island, promoting enhanced vertical mixing through the water column. This enhanced mixing can result in elevated surface-dissolved Fe concentrations around the Pribilof Islands, likely from the combined entrainment of both Fe-rich bottom shelf waters and shelf sediments. For example, Aguilar-Islas et al. (2007) observed elevated dissolved Fe concentrations (~5–6 nmol L^{-1}) in this region, which fueled productivity in adjacent Green Belt waters. Similarly, surface-dissolved Fe concentrations were also elevated near the Aleutian Islands (~1 nmol L^{-1}) where tidal forcing and island bathymetry promotes deep vertical mixing. However, the dissolved Fe concentrations observed near these islands were not nearly as high as near the Pribilof Islands, and the difference is attributed to the lack of continental shelf input of sedimentary iron around the Aleutian Islands (Aguilar-Islas et al. 2007).

From previous work we know that the physicochemical speciation of dissolved Fe plays a critical role in the solubility and supply of dissolved Fe in other coastal environments such that dissolved Fe concentrations do not generally exceed the stronger (L_1) ligand class's concentrations regardless of the amount of readily dissolvable particulate Fe (Buck et al. 2007). In the absence of organic ligands, the inorganic solubility of Fe(III) in pH 8 seawater is low (0.08 nmol L^{-1}) (Wu et al. 2001), resulting in concentrations that would limit the growth of most large phytoplankton. However, these ligands appear ubiquitously present in the marine environment, with stronger L_1 ligands generally complexing >99% of the total dissolved Fe in a given environment.

Here we present the ambient physicochemical speciation of dissolved Fe in surface and subsurface waters of the deep basin and continental shelf domains of the southeastern Bering Sea and along the Aleutian Archipelago, from August and September 2003. Our objectives for this study were to determine the extent of ambient complexation of dissolved Fe by organic ligands across the natural dissolved Fe concentration gradient of the Bering Sea basin–shelf–island system, and to evaluate the distribution patterns and the role of these ligands in this productive ecosystem.

Methods

Sample collection—Underway nutrient and hydrographic samples were collected from the ship's flow-through seawater system while subsurface samples were collected using an instrumental rosette that included a Seabird conductivity-temperature-depth (CTD) system equipped with a fluorometer. As the CTD fluorometer had been calibrated with chlorophyll *a* (Chl *a*) values for a ratio of relative fluorescence units (RFU) to Chl *a* (RFU/Chl *a* = 0.90, r^2 = 0.73, n = 16), subsurface fluorescence is presented in the calibrated RFU units while surface fluorescence is presented in volts. Surface and subsurface samples were analyzed for macronutrients (nitrite + nitrate, silicic acid, phosphate) on a Lachat QuickChem 8000™ flow injection analysis system following standard protocols (Parsons et al. 1984). The complete data set of these nutrients is published elsewhere (Aguilar-Islas et al. 2007), with only the nitrate + nitrite (hereafter referred to as nitrate) data presented here.

A trace-metal clean surface pump ''sipper'' system (Bruland et al. 2005) was used to collect dissolved Fe speciation samples underway along surface transects in the

southeastern Bering Sea from 11 August to 05 September 2003 aboard the RV *Kilo Moana* (Fig. 1). Subsurface speciation samples were collected at stations using 30-liter Teflon™-coated GO-Flo™ bottles (General Oceanics) on a Kevlar™ hydroline (Bruland et al. 1979). Upon collection, all surface speciation samples were filtered through cleaned (Bruland et al. 2005) 0.45-μm absolute pore size Teflon membrane polypropylene capsule filters (Calyx™, MSI). Subsurface speciation samples were filtered through cleaned (Bruland et al. 2005) 142-mm-diameter 0.4-μm absolute pore size polycarbonate track-etched membrane filters (Nuclepore™, Whatman) held in polytetrafluoroethylene (PTFE) Teflon filter sandwiches (Millipore).

Total dissolved Fe analyses—After collection, filtered total dissolved Fe samples were acidified to pH ~1.7 with quartz-distilled 6 mol L^{-1} hydrochloric acid. Total dissolved Fe analyses were conducted in our shore-based laboratory using sector–field inductively coupled plasma mass spectrometry with either a nitriloacetic acid preconcentration column at low (~1.7) pH (Lohan et al. 2006) or an iminodiacetate column at pH 5.5 after ultraviolet oxidation of ambient Fe-binding ligands (Hurst and Bruland 2007). These methods and the complete total dissolved Fe results from the Bering Sea are published elsewhere (Aguilar-Islas et al. 2007), with a subset that was utilized for dissolved Fe speciation analyses included here.

Dissolved Fe speciation analyses—Speciation samples were frozen after collection at sea and returned to the shore-based laboratory where they were thawed and vigorously shaken before analysis. The physicochemical speciation of dissolved Fe was then measured with a competitive ligand exchange–adsorptive cathodic stripping voltammetry (CLE-ACSV) method using salicylaldoxime (SA) as the added ligand (Buck et al. 2007). We used an SA concentration of 25 μmol L^{-1} and the calibrated log $\beta^{cond}_{Fe(SA)_2Fe'}$ of 11.1 in the analyses of all of our surface and subsurface speciation samples from the Bering Sea, as detailed in Buck et al. (2007).

The concentrations and conditional stability constants of ambient Fe-binding ligand classes were then determined from the raw speciation data using van den Berg/Ruzic and Scatchard transformations (Rue and Bruland 1995; Ruzic 1982). Two ligand classes were observed in all of these samples and can be interpreted as averages of a continuum of ambient Fe-binding organic matter within the analytical window, with the L_1 ligand class representing the stronger Fe-binding ligands and the L_2 ligand class the weaker Fe-binding ligands. This method, and the theory behind it, are detailed elsewhere (Rue and Bruland 1995; Buck et al. 2007).

Results

Transects—Surface and subsurface speciation samples were collected along three transects in the southeastern Bering Sea (Fig. 1). Underway surface speciation sample stations are named by the surface transect (e.g., N.no.) and order of collection along the transect line (e.g., N.1 denotes first surface speciation sample collected along transect N). Subsurface sample stations are simply numbered, and correspond to the station numbers reported in Aguilar-Islas et al. (2007). Transects N and M, the northernmost and middle transects, respectively, were cross-shelf transects that covered all three continental shelf domains, the shelf break, and the deep basin. Transect N additionally passed between the Pribilof Islands, whereas transect M did not include any island samples. Transect A, the Aleutian Archipelago transect, encompassed the Bering Canyon and eastern Aleutian Islands and was further subdivided into transects A1, A2, and A3 (Fig. 1). Dissolved Fe speciation samples were obtained along all transects, and subsurface samples were obtained at stations located along each transect (Fig. 1). Surface speciation results from this work, along with transect dissolved Fe and nitrate concentrations from this cruise (published in Aguilar-Islas et al. 2007), have been plotted in Fig. 2 for transect N and transect M, and in Fig. 3A–C for transect A.

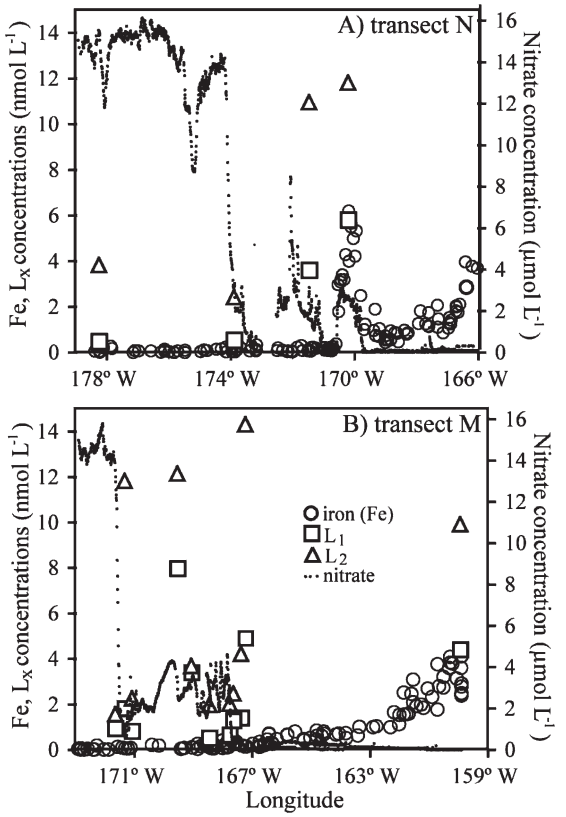

Fig. 2. Dissolved Fe, L_1 ligand, and total ($[L_1] + [L_2]$) ligand concentrations, along with nitrate concentrations, for (A) transect N and for (B) transect M. Complete dissolved Fe and nitrate data sets available from Aguilar-Islas et al. (2007).

The hydrographic characteristics of the Bering Sea surface and subsurface speciation samples are detailed in Table 1 and results from the speciation analyses are provided in Table 2. These speciation samples are complementary to more extensive dissolved Fe and hydrographic data also obtained from this region and published

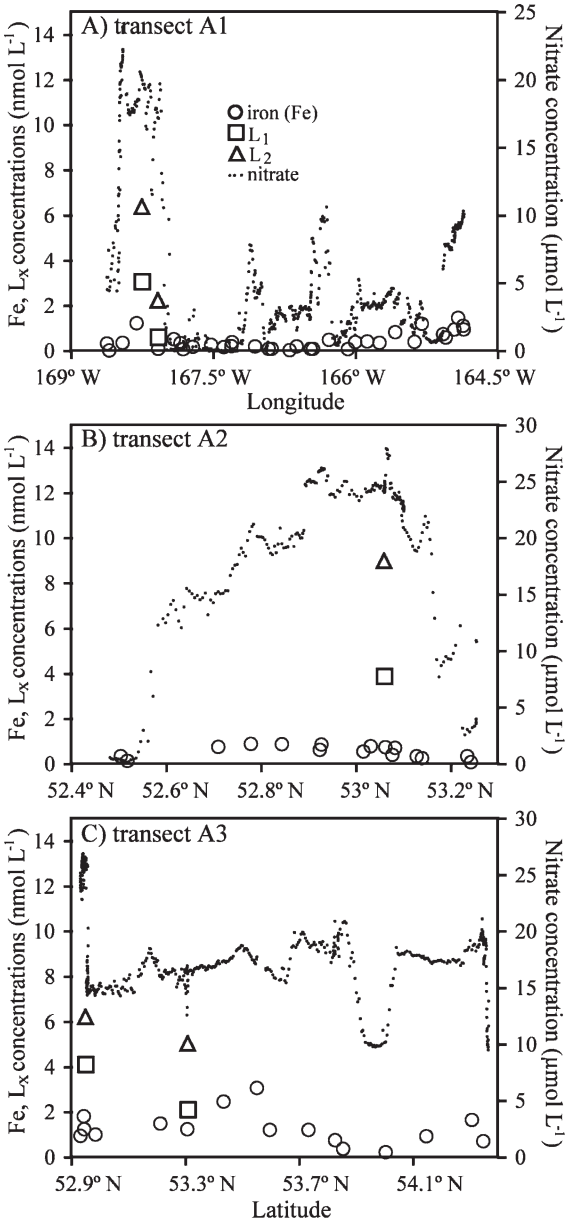

Fig. 3. (A) Transect A1, (B) transect A2, and (C) transect A3 dissolved Fe, L_1 ligand, and total ($[L_1] + [L_2]$) ligand concentrations, along with nitrate concentrations. Complete dissolved Fe and nitrate data sets available from Aguilar-Islas et al. (2007).

elsewhere (Aguilar-Islas et al. 2007). Here we present a subset of that data to contextualize our speciation data.

Two ligand classes were distinguished in all of the speciation samples (Table 2). The measured stability constants for the stronger L_1-type ligands ($K^{cond}_{FeL_1,Fe'}$) and the weaker L_2-type ligands ($K^{cond}_{FeL_2,Fe'}$) were comparable between the surface and subsurface samples. In the surface samples, $K^{cond}_{FeL_1,Fe'}$ ranged from $10^{11.1}$ to $10^{12.0}$ mol L^{-1} equivalents with a mean log $K^{cond}_{FeL_1,Fe'}$ of 11.5 ± 0.3, and from $10^{11.1}$ to $10^{11.8}$ mol L^{-1} equivalents with a mean log $K^{cond}_{FeL_1,Fe'}$ of 11.4 ± 0.3 in the subsurface samples (Table 2). For the weaker L_2 ligands, $K^{cond}_{FeL_2,Fe'}$ ranged from $10^{9.7}$ to $10^{10.8}$ mol L^{-1} equivalents with a mean log $K^{cond}_{FeL_2,Fe'}$ of 10.3 ± 0.3 in surface samples and from $10^{9.9}$ to $10^{10.5}$ mol L^{-1} equivalents with a mean log $K^{cond}_{FeL_2,Fe'}$ of 10.2 ± 0.2 in the subsurface samples (Table 2).

[Fe] versus [L_1]—As shown in Fig. 4, the dissolved Fe and ambient L_1 ligand concentrations were correlated (r^2 = 0.86, n = 18; $p < 0.001$; simple linear regression) in all surface and subsurface speciation samples where dissolved Fe concentrations were at least 0.2 nmol L^{-1}. Below a dissolved Fe concentration of 0.2 nmol L^{-1} large excesses in L_1 concentrations were measured, and these values deviated from the correlation observed at higher concentrations (Fig. 4). A 1 : 1 ($y = x$) line plotted in Fig. 4 also demonstrates that while dissolved Fe concentrations approach the L_1 ligand concentrations, they do not appreciably exceed them.

There was a much poorer correlation between dissolved Fe concentrations and the weaker ambient L_2 ligand concentrations (r^2 = 0.63; Fig. 4). These weaker L_2-type ligands were detected in all of our speciation samples from the Bering Sea, with an excess of these weaker ligands over dissolved Fe concentrations. Further, at the lower dissolved Fe concentrations (<0.2 nmol L^{-1}) the weaker L_2 ligands, like the stronger L_1-type ligands, were present in larger and more variable excesses beyond dissolved Fe.

Inner shelf domain—Subsurface Stas. 17 and 18, as well as surface Sta. M.1, were located within the inner shelf domain shoreward of the 50-m isobath (Fig. 1). All of these samples were collected along transect M, although the inner shelf domain of this transect presented some hydrographic structure due to warm and calm conditions (Aguilar-Islas et al. 2007). Dissolved Fe and ligand concentrations were elevated in this region, with Sta. 17 presenting the highest dissolved Fe (13 nmol L^{-1}), L_1 (17 nmol L^{-1}), and L_2 (14 nmol L^{-1}) concentrations at a depth of 35 m (bottom depth ~50 m). Surface Sta. M.1 was located within Bristol Bay in relatively warm (12°C) and low-salinity (S = 29.6) water. Dissolved Fe and ligand concentrations were elevated in this surface sample ([Fe] = 3.6 nmol L^{-1}; $[L_1]$ = 4.4 nmol L^{-1}; $[L_2]$ = 5.5 nmol L^{-1}; Fig. 2).

Middle shelf domain—Subsurface Stas. 19, 20, and 22 were located in the middle shelf domain, and these samples were all taken along transect M. Stas. 19 and 20 were in the middle of this domain, while Sta. 22 was near the middle shelf front at the 100-m isobath. Dissolved Fe and ligand concentrations were elevated in the subsurface samples of Stas. 19 ([Fe] = 3.7 nmol L^{-1}; $[L_1]$ = 3.8 nmol L^{-1}; $[L_2]$ = 4.7 nmol L^{-1}) and 20 ([Fe] = 4.5 nmol L^{-1}; $[L_1]$ = 9.9 nmol L^{-1}; $[L_2]$ = 3.9 nmol L^{-1}), with higher concentrations ([Fe] = 5.1 nmol L^{-1}; $[L_1]$ = 5.3 nmol L^{-1}; $[L_2]$ = 15 nmol L^{-1}) observed at Sta. 22 (Table 2). One surface speciation station from transect N was located in the middle shelf domain, Sta. N.4, although this station was near St. Paul Island and was likely in the well-mixed coastal domain surrounding the island. This surface station presented the highest dissolved Fe (6.2 nmol L^{-1}) and L_1 (5.8 nmol L^{-1}) concentrations of the surface samples. This

Table 1. Hydrographic and station location data for all samples.

Sta.	Date	Depth	Lat (°N)	Long (°W)	*T* (°C)	S	N* (μmol L^{-1})
17	24 Aug 03	35 m	58.103	160.746	8.18	31.60	0.31
18	24 Aug 03	35 m	57.532	162.009	8.08	31.66	0.6
19	24 Aug 03	40 m	56.069	163.191	5.33	31.78	9.39
20	24 Aug 03	45 m	56.747	164.062	3.66	31.89	8.52
22	25 Aug 03	50 m	56.179	165.524	3.89	31.91	18.5
38	02 Sep 03	50 m	54.193	167.071	6.72	32.98	19.2
42	04 Sep 03	10 m	52.932	169.369	6.27	33.03	22.9
42	04 Sep 03	30 m	52.932	169.369	6.21	33.07	24.9
42	04 Sep 03	57 m	52.932	169.369	5.71	33.19	25.4
N.1	13 Aug 03	Surface	55.040	178.239	10.79	33.02	15.46
N.2	15 Aug 03	Surface	55.550	173.873	10.61	32.53	3.31
N.3	17 Aug 03	Surface	56.425	171.454	10.15	32.51	2.05
N.4	18 Aug 03	Surface	57.138	170.193	9.66	31.83	2.69
M.1	22 Aug 03	Surface	58.310	159.931	12.04	29.60	bld†
M.2	27 Aug 03	Surface	55.497	167.214	10.98	31.81	bld†
M.3	27 Aug 03	Surface	55.435	167.368	10.79	31.88	0.34
M.4	27 Aug 03	Surface	55.329	167.621	10.77	31.93	0.37
M.5	27 Aug 03	Surface	55.288	167.753	10.15	32.26	1.93
M.6	29 Aug 03	Surface	55.134	168.435	10.42	32.34	3.00
M.7	29 Aug 03	Surface	54.983	169.048	10.24	32.38	3.40
M.8	29 Aug 03	Surface	54.441	171.312	10.39	32.50	0.62
A1.1	02 Sep 03	Surface	53.889	168.080	8.21	32.51	17.16
A1.2	02 Sep 03	Surface	53.834	168.250	6.97	32.60	20.0
A2.1	03 Sep 03	Surface	53.060	169.821	6.14	32.87	24.55
A3.1	04 Sep 03	Surface	53.307	168.576	7.59	32.33	16.39

* Complete nitrate data set published in Aguilar-Islas et al. (2007).
† bld indicates that concentrations were below the limit of detection of the analyzer.

Table 2. Speciation results for all samples. Ligand concentrations are presented as the mean and standard deviation from van den Berg/Ruzic and Scatchard linearization results. Complete dissolved Fe and fluorescence data set published in Aguilar-Islas et al. (2007). Sample precision for dissolved Fe measurements ranged from <3% RSD at high (>1 nmol L^{-1}) concentrations to <7% RSD at lower concentrations.

Sta.	[Fe] (nmol L^{-1})	[L_1] (nmol L^{-1})	log K_1	[L_2] (nmol L^{-1})	log K_2	Fluor*
17	13	18±1	11.4	14±1	10.2	1.14
18	4.2	5.8±0.1	11.3	6.9±0.1	10.3	1.07
19	3.7	3.8±0.1	11.3	4.7±0.2	10.4	0.46
20	4.5	9.9±0.1	11.8	3.9±0.1	10.5	0.12
22	5.1	5.3±0.1	11.8	15±1	9.9	0.11
38	0.76	2.0±0.1	11.1	2.7±0.1	10.3	0.78
42-10m	1.9	1.5±0.1	11.4	4.0±0.1	10.0	0.86
42-30m	1.6	1.6±0.1	11.2	2.8± 0.1	10.4	0.65
42-57m	3.1	7.0±0.1	11.3	8.5±0.3	10.0	0.66
N.1	0.01	0.46±0.01	11.5	3.3±0.1	9.7	0.11
N.2	0.11	0.52±0.01	11.7	1.9±0.1	10.0	0.46
N.3	0.13	3.6±0.1	11.1	7.4±0.1	10.0	nda†
N.4	6.2	5.8±0.2	11.2	6.0±0.2	10.0	0.39
M.1	3.6	4.4±0.3	11.5	5.5±0.2	10.4	0.42
M.2	0.15	4.9±0.2	11.5	9.4±0.6	10.6	0.58
M.3	0.19	1.4±0.3	11.4	2.8±0.3	10.3	0.58
M.4	0.27	1.3±0.1	11.1	1.2±0.1	10.5	0.58
M.5	0.43	0.64±0.01	11.8	1.4±0.1	10.4	0.52
M.6	0.20	0.43±0.01	11.5	1.5±0.1	9.8	1.70
M.7	0.12	3.8±0.1	11.9	1.8±0.1	10.6	1.76
M.8	0.08	1.8±0.1	11.7	5.8±0.1	10.8	2.77
A1.1	0.1	0.60±0.1	11.8	1.6±0.1	9.9	0.40
A1.2	1.2	3.1±0.1	12.0	3.3±0.1	10.5	0.25
A2.1	0.75	3.9±0.1	11.3	5.1±0.3	10.4	0.24
A3.1	1.3	2.1±0.1	11.3	2.9±0.1	10.5	0.30

* Subsurface fluorescence data is in units of RFU and surface fluorescence data is in units of volts.
† nda indicates no data available at this station.

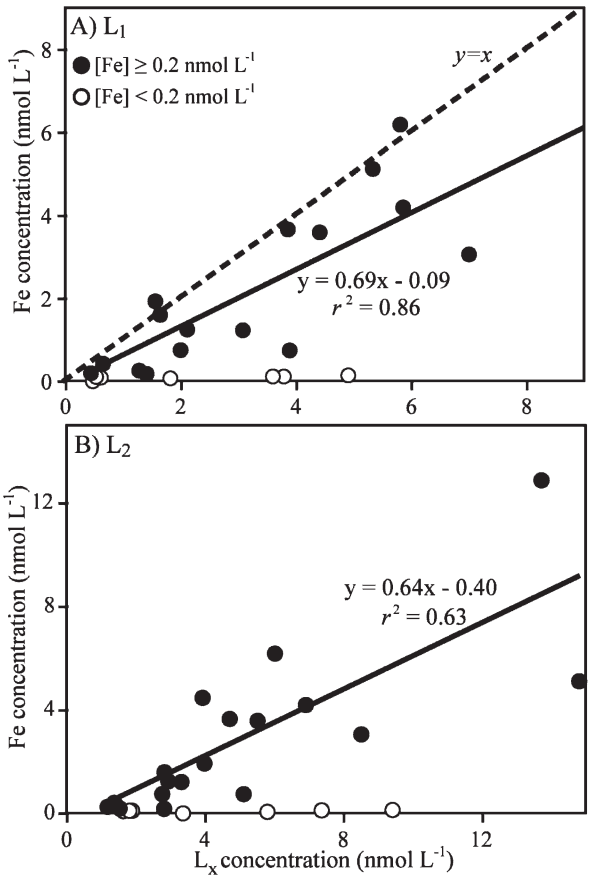

Fig. 4. The concentrations of dissolved Fe as a function of (A) the stronger L_1-type ligand concentrations and of (B) the weaker L_2-type ligand concentrations for all speciation samples from the southeastern Bering Sea at dissolved Fe concentrations of at least 0.2 nmol L^{-1} (closed circles) and below 0.2 nmol L^{-1} (open circles). The dashed line represents $y = x$, and the solid line a simple linear regression of the data represented by closed circles.

was also the only surface speciation sample where dissolved Fe slightly exceeded the stronger L_1 ligand class (Fig. 2).

Outer shelf domain—Surface speciation Stas. M.2, M.3, and M.4 from transect M and N.3 from transect N were located within the outer shelf domain. No subsurface samples were collected for Fe speciation in the outer shelf domain. Sta. N.3 was located near the shelf break front and presented low dissolved Fe concentrations (0.13 nmol L^{-1}) with large concentrations of L_1 (3.6 nmol L^{-1}) and L_2 (7.4 nmol L^{-1}) (Table 2). Along transect M, a general gradient in dissolved Fe, L_1, and L_2 was observed in this domain (samples M.2, M.3, and M.4), with increasing concentrations of dissolved Fe ([Fe] = 0.15 to 0.27 nmol L^{-1}) and decreasing concentrations of ambient ligands ([L_1] = 4.9 to 1.3 nmol L^{-1}; [L_2] = 9.4 to 1.2 nmol L^{-1}) (Fig. 2).

Oceanic domain—The remaining surface samples from transect N (N.1, N.2) and from transect M (M.5, M.6, M.7, M.8) were all collected from the oceanic domain of the southeastern Bering Sea (Fig. 1). Sample N.1 was the only surface station located within the HNLC Bering Sea gyre, and presented high nitrate concentrations (15 μmol L^{-1}), extremely low dissolved Fe (~0.01 nmol L^{-1}), and excesses of both L_1 (0.46 nmol L^{-1}) and L_2 (3.3 nmol L^{-1}) ligand concentrations (Fig. 2). In general, dissolved Fe and L_1 ligand concentrations decreased from the outer shelf basin westward while the weaker L_2 ligand concentrations increased (Fig. 2). At dissolved Fe concentrations less than 0.2 nmol L^{-1} L_1 ligand concentrations were generally elevated over [Fe] (Table 2), although the concentrations of L_1 ligands were less elevated in the oceanic domain (~0.5 nmol L^{-1}; Table 2) than in the outer shelf domain (~3 nmol L^{-1} ; Table 2).

Aleutian Archipelago—Surface speciation Stas. A1.1, A1.2, A2.1, and A3.1, as well as subsurface Stas. 38 and 42, were all located in the vicinity of the Aleutian Islands along transects A1–3 (Fig. 1). With the exception of sample A1.1, dissolved Fe and ligand concentrations were elevated in all of these samples (Fig. 3). The deepest sample (57 m) from Sta. 42 presented the highest dissolved Fe (3.1 nmol L^{-1}) and ligand ([L_1] = 7.0 nmol L^{-1}, [L_2] = 8.5 nmol L^{-1}) concentrations (Table 2).

Discussion

In this work, we have shown that a strong correlation (r^2 = 0.86, n = 18, $p < 0.001$; simple linear regression) exists between dissolved Fe and L_1 concentrations in surface and subsurface waters over the Bering Sea shelf and near external sources of Fe where elevated (>0.2 nmol L^{-1}) dissolved Fe concentrations persist (Fig. 4). There was no such correlation observed between dissolved Fe and weaker L_2 ligand concentrations (Fig. 4) or between dissolved L_1 and nitrate concentrations (Tables 1, 2). Previous work has documented a similarly strong correlation (r^2 = 0.84, n = 14, $p < 0.001$; simple linear regression) between dissolved Fe and L_1 ligand concentrations in surface waters of river plume, estuary outflow, and coastal systems over a range of intermediate dissolved Fe concentrations from 0.6–8 nmol L^{-1} (Buck et al. 2007). The cohesion between these speciation results supports the idea that the stronger L_1 ligands, and not the weaker L_2 ligands, play a crucial role in the solubility, and, therefore, likely the bioavailability of dissolved Fe in the marine environment.

In Fig. 5 we further show that this relation is not unique to the Bering Sea and coastal NE Pacific, or even to the specific CLE-ACSV methodology (using SA) reported here, by including published speciation results from several other CLE-ACSV studies: Rue and Bruland (1995, 1997), Gledhill et al. (1998), Powell and Wilson-Finelli (2003*a*), Boye et al. (2003), Cullen et al. (2006), and Buck et al. (2007). In this figure we again see a strong relation (r^2 = 0.86, n = 103, $p < 0.001$; simple linear regression) for all of these studies between dissolved Fe and L_1 concentrations at intermediate dissolved Fe concentrations of at least 0.2 nmol L^{-1}. Although we recognize that correlation in this case is not necessarily indicative of causation, the strong relation between dissolved Fe and only L_1 ligand

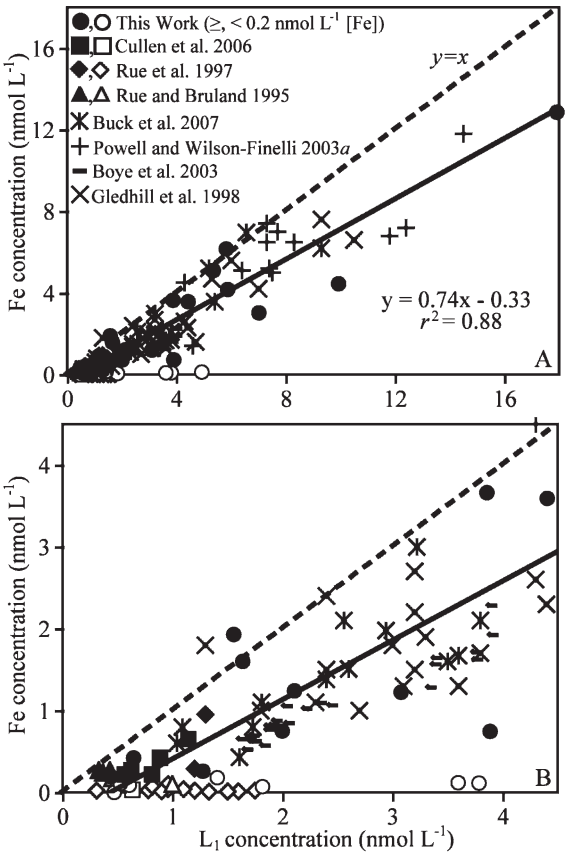

Fig. 5. (A) Complete plot and (B) and expanded plot of dissolved Fe concentrations as a function of L_1 ligand concentrations for this work and several published studies, excluding estuarine, river mouth, and bottom boundary layer data. Samples with dissolved Fe concentrations of at least 0.2 nmol L^{-1} (closed symbols) and samples with dissolved Fe concentrations below 0.2 nmol L^{-1} (open symbols) are both represented. The dashed line represents $y = x$, and the solid line a simple linear regression of the data represented by all of the closed symbols.

concentrations observed in this data set is compelling evidence for a governing role by L_1 in the solubility and bioavailability of dissolved Fe. The strong correlation between Fe and L_1 may also suggest that dissolved Fe is required for the production of these L_1-type ligands.

As done for the correlation in Buck et al. (2007), estuarine, river mouth, and bottom boundary layer values were excluded from the data set as these samples were somewhat rare (only seen in Powell and Wilson-Finelli 2003*a*, Buck et al. 2007). In these samples dissolved Fe concentrations were greatly elevated (up to ~22 nmol L^{-1} [Fe]) along with even larger excesses of L_1 ligands (up to ~56 nmol L^{-1} [L_1]). Speciation results for dissolved Fe concentrations below 0.2 nmol L^{-1} are, however, included in Fig. 5, and as for the data in Fig. 4, a disproportionate excess of L_1 ligands with respect to dissolved Fe concentrations is observed in these results.

In our data from the oceanic domain of the Bering Sea, while L_1 ligands are in excess of the low (<0.2 nmol L^{-1}) dissolved Fe, concentrations of L_1 remain low (~0.5 nmol L^{-1}; Table 2) in this HNLC region. Similarly, relatively low L_1 ligand concentrations ([L_1] = 0.32 nmol L^{-1}; Fig. 5) were also observed in the Fe-limited waters (<0.2 nmol L^{-1}) of the Equatorial Pacific (Rue and Bruland 1997). In contrast, along the outer shelf break of the Bering Sea, in the productive Green Belt region, dissolved Fe concentrations are also low (<0.2 nmol L^{-1}), and L_1 concentrations are much higher (~3 nmol L^{-1}). These elevated L_1 ligand concentrations are similar to those observed in adjacent high-Fe shelf waters ([L_1] = ~5 nmol L^{-1}).

The excesses of L_1 ligand concentrations over dissolved Fe concentrations observed in samples with low (<0.2 nmol L^{-1}) dissolved Fe may be due to the removal of Fe from the FeL_1 complex via biological uptake. As an example, eukaryotic phytoplankton have been shown to reduce Fe from ambient $Fe(III)L_1$ organic complexes, allowing Fe(II) to dissociate, and subsequently take up the Fe into the cell—presumably leaving the Fe-binding organic ligands behind (Maldonado and Price 2001). In incubation experiments conducted in the Bering Sea, ambient dissolved Fe was readily taken up (Aguilar-Islas et al. 2007; Hurst and Bruland 2007), and speciation measurements in these waters demonstrated that >99% of the dissolved Fe was complexed by L_1 ligands (this work). Further, our data reveal that dissolved Fe is supplied to the surface waters of the productive Green Belt region from adjacent shelf waters as strong FeL_1 complexes, and within this boundary region dissolved Fe is depleted to low (<0.2 nmol L^{-1}) levels by surface phytoplankton while L_1 ligand concentrations remain elevated (~3 nmol L^{-1}; Table 2). Thus, it appears that dissolved Fe in the Bering Sea, which is strongly complexed by L_1 ligands, is readily available to ambient phytoplankton communities. If indeed the uptake of Fe is reflected in increasing excesses of L_1 left behind, then the concentration of L_1 ligands in these waters may represent the amount of Fe originally supplied.

While the sources and identity of L_1 ligands in general remain poorly understood, some authors have suggested that ambient strong Fe-binding ligands resemble siderophores (Witter et al. 2000; Macrellis et al. 2001). As siderophores are produced by marine microorganisms to access Fe from their surrounding environment, the large excess of L_1 observed at very low (<0.2 nmol L^{-1}) dissolved Fe concentrations (Table 2, Figs. 4, 5) might support the possibility of some fraction of L_1 ligands being siderophores. In the oceanic domain and Green Belt regions of the outer shelf domains, the combination of low dissolved Fe concentrations and elevated L_1 ligand concentrations is coincident with observed Fe stress, and, in some cases, Fe limitation (Aguilar-Islas et al. 2007). The possible production of siderophores in response to Fe stress in these low-Fe waters of the Bering Sea would be consistent with laboratory results (Wilhelm and Trick 1994; Borer et al. 2005). However, this type of response has yet to be observed in the field. In fact, Rue and Bruland (1997) showed that in the IronExII experiment strong Fe-binding ligands were produced in response to iron additions. From this work, we cannot determine whether the excess of L_1 seen in our low-Fe samples is due to L_1

production under Fe-stressing or Fe-limiting conditions or due to Fe being reduced from the FeL_1 complexes and taken up, leaving L_1 behind.

The elevated concentrations of both L_1 and L_2 observed in subsurface waters (Table 2) over the shelf indicate that shelf sediments likely serve as a source of these Fe-binding ligands. These L_1 and L_2 ligands may originate from Fe-binding organic matter adsorbed to inorganic Fe oxide colloids resuspended from the shelf sediments. The ligands can be released to pore waters as the Fe oxides they are associated with are reduced in the sediments, allowing these ligands to diffuse into the overlying water column. These ligands may also remain associated with colloids throughout the water column. The presence of both stronger and weaker ligands in subsurface waters suggests that these ligands are not rapidly degraded in the water column, at least at depth. An additional source of ligands within the subsurface waters could be from the degradation of the export flux of organic material (e.g., cell wall proteins, fragments).

The lower ligand concentrations generally measured in surface waters of the Bering Sea may be the result of the photoreactivity of these ligands. Laboratory and fieldwork have both documented the photochemical degradation of Fe-binding ligands in seawater (Barbeau et al. 2001; Powell and Wilson-Finelli 2003*b*). However, any photochemical degradation of ligands in surface waters was not reflected in Fe-binding stability constants of the ligands measured, as no distinguishable difference was observed between surface and subsurface conditional stability constants for either L_1 or L_2 ligands (Table 2).

The seemingly ubiquitous nature of the correlation between dissolved Fe and L_1 concentrations suggests that this particular ligand class plays a governing role in the solubility and supply of Fe to the marine environment. The identity of these L_1 ligands remains speculative, although the conditional stability constants of these ligands are similar to those of isolated marine siderophores in coastal waters (Macrellis et al. 2001). Other possibilities for these ligands include macromolecules like polysaccharides, organic colloids, or a fraction of the uncharacterized component of dissolved organic carbon. Regardless of their source, these ligands appear to control dissolved Fe concentrations and must be considered in examining the biogeochemical cycling of Fe in the marine environment.

References

Aguilar-Islas, A. M., M. P. Hurst, K. N. Buck, B. Sohst, G. J. Smith, M. C. Lohan, and K. W. Bruland. 2007. Micro- and macronutrients in the southeastern Bering Sea: Insight into iron-replete and iron-deplete regimes. Prog. Oceanogr. **72:** 99–126.

Barbeau, K. A., E. L. Rue, K. W. Bruland, and A. Butler. 2001. Photochemical cycling of iron in the surface ocean mediated by microbial iron (III)-binding ligands. Nature **413:** 409–413.

Borer, P. M., B. Sulzberger, P. Reichard, and S. M. Kraemer. 2005. Effect of siderophores on the light-induced dissolution of colloidal iron(III) (hydr)oxides. Mar. Chem. **93:** 179–193.

Boye, M. B., A. P. Aldrich, C. M. G. van den berg, J. T. M. de Jong, M. J. W. Veldhuis, and H. J. W. de Baar. 2003. Horizontal gradient of the chemical speciation of iron in surface waters of N.E. Atlantic Ocean. Mar. Chem. **80:** 129–143.

Bruland, K. W., R. P. Franks, G. A. Knauer, and J. H. Martin. 1979. Sampling and analytical methods for the determination of copper, cadmium, zinc and nickel at nanogram per litre level in seawater. Anal. Chim. Acta **105:** 233–245.

———, E. L. Rue, G. Smith, and G. R. Ditullio. 2005. Iron, macronutrients and diatom blooms in the Peru upwelling regime: Brown waters of Peru versus blue waters. Mar. Chem. **93:** 81–103.

Buck, K. N., M. C. Lohan, C. J. M. Berger, and K. W. Bruland. 2007. Dissolved iron speciation in two distinct river plumes and an estuary: Implications for riverine iron supply. Limnol. Oceanogr. **52:** 843–855.

Coachman, L. K., and R. L. Charnell. 1979. On lateral water mass interaction—a case study, Bristol Bay, Alaska. J. Phys. Oceanogr. **9:** 278–297.

Cullen, J. T., B. A. Bergquist, and J. W. Moffett. 2006. Thermodynamic characterization of the partitioning of iron between soluble and colloidal species in the Atlantic Ocean. Mar. Chem. **98:** 295–303.

Gledhill, M., C. M. G. van den Berg, R. F. Nolting, and K. R. Timmermans. 1998. Variability in the speciation of iron in the northern North Sea. Mar. Chem. **59:** 283–300.

Hurst, M. P., and K. W. Bruland. 2007. An investigation into the exchange of iron and zinc between soluble, colloidal, and particulate size-fractions in shelf waters using low-abundance isotopes as tracers in shipboard incubation experiments. Mar. Chem. **103:** 211–226.

Leblanc, K., and others. 2005. Fe and Zn effects on the Si cycle and diatom community structure in two contrasting high and low-silicate HNLC areas. Deep-Sea Res. I **52:** 1842–1864.

Liu, H., K. Suzuki, and T. Saino. 2002. Phytoplankton growth and microzooplankton grazing in the subarctic Pacific Ocean and the Bering Sea during summer 1999. Deep-Sea Res. I **49:** 363–375.

Lohan, M. C., A. M. Aguilar-Islas, and K. W. Bruland. 2006. Direct determination of iron in acidified (pH 1.7) seawater samples by flow injection analysis with catalytic spectrophotometric detection: Application and intercomparison. Limnol. Oceanogr. Methods **4:** 164–171.

Macrellis, H. M., C. G. Trick, E. L. Rue, G. Smith, and K. W. Bruland. 2001. Collection and detection of natural iron-binding ligands from seawater. Mar. Chem. **76:** 175–187.

Maldonado, M. T., and N. M. Price. 2001. Reduction and transport of organically bound iron by *Thalassiosira oceanica* (Bacillariophyceae). J. Phycol. **37:** 298–310.

Mordy, C. W., P. J. Stabeno, C. Ladd, S. Zeeman, D. P. Wisegarver, S. A. Salo, and G. L. Hunt. 2005. Nutrients and primary production along the eastern Aleutian Island Archipelago. Fish. Oceanogr. **14:** 55–76.

Parsons, T. R., Y. Maita, and C. M. Lalli. 1984. A manual of chemical and biological methods for seawater analysis., Pergamon Press.

Peers, G., S.-A. Quesnel, and N. M. Price. 2005. Copper requirements for iron acquisition and growth of coastal and oceanic diatoms. Limnol. Oceanogr. **50:** 1149–1158.

Powell, R. T., and A. Wilson-Finelli. 2003a. Importance of organic Fe complexing ligands in the Mississippi River plume. Estuar. Coastal Shelf Sci. **58:** 757–763.

———, and A. Wilson-Finelli. 2003b. Photochemical degradation of organic iron complexing ligands in seawater. Aquat. Sci. **65:** 367–374.

RUE, E. L., AND K. W. BRULAND. 1995. Complexation of iron(III) by natural organic ligands in the Central North Pacific as determined by a new competitive ligand equilibration adsorptive cathodic stripping voltammetric method. Mar. Chem. **50:** 117–138.

———, AND ———. 1997. The role of organic complexation on ambient iron chemistry in the equatorial Pacific Ocean and the response of a mesoscale iron addition experiment. Limnol. Oceanogr. **42:** 901–910.

RUZIC, I. 1982. Waters and its information for trace metal speciation. Anal. Chim. Acta **140:** 99–113.

SHIOMOTO, A. 1999. Effect of nutrients on phytoplankton size in the Bering Sea basin, p. 323–340. *In* T. R. Loughlin and K. Ohtani [eds.], Dynamics of the Bering Sea. University of Alaska Sea Grant.

SPRINGER, A. M., C. P. MCROY, AND M. V. FLINT. 1996. The Bering Sea Green Belt: Shelf edge processes and ecosystem production. Fish. Oceanogr. **5:** 205–223.

STABENO, P. J., J. D. SCHUMACHER, S. A. SALO, G. L. HUNT JR., AND M. FLINT. 1999. Physical environment around the Pribilof Islands, p. 193–216. *In* T. R. Loughlin and K. Ohtani [eds.], Dynamics of the Bering Sea. University of Alaska Sea Grant.

SUKHANOVA, I. N., H. J. SEMINA, AND M. V. VENTTSEL. 1999. Spatial distribution and temporal variability of phytoplankton in the Bering Sea, p. 453–484. *In* T. R. Loughlin and K. Ohtani [eds.], Dynamics of the Bering Sea. University of Alaska Sea Grant.

WHITLEDGE, T. E., AND V. A. LUCHIN. 1999. Summary of chemical distributions and dynamics in the Bering Sea, p. 217–250. *In* T. R. Loughlin and K. Ohtani [eds.], Dynamics of the Bering Sea. University of Alaska Fairbanks.

WILHELM, S., AND C. G. TRICK. 1994. Iron-limited growth of cyanobacteria: Multiple siderophore production is a common response. Limnol. Oceanogr. **39:** 1979–1984.

WITTER, A. E., D. A. HUTCHINS, A. BUTLER, AND G. W. LUTHER. 2000. Determination of conditional stability constants and kinetic constants for strong model Fe-binding ligands in seawater. Mar. Chem. **69:** 1–17.

WU, J., E. BOYLE, W. SUNDA, AND L.-S. WEN. 2001. Soluble and colloidal iron in the oligotrophic North Atlantic and North Pacific. Science **293:** 847–849.

Received: 20 November 2006
Accepted: 29 April 2007
Amended: 16 May 2007